

**DESIGN AND DEVELOPMENT OF ENERGY EFFICIENT  
SINGLE PHASE INDUCTION MOTOR FOR FAN  
APPLICATIONS**

**UTKARSH SHARMA**



**DEPARTMENT OF ELECTRICAL ENGINEERING  
INDIAN INSTITUTE OF TECHNOLOGY DELHI  
NOVEMBER 2021**

© Indian Institute of Technology Delhi (IITD), New Delhi, 2021

**DESIGN AND DEVELOPMENT OF ENERGY EFFICIENT  
SINGLE PHASE INDUCTION MOTOR FOR FAN  
APPLICATIONS**

*by*

**UTKARSH SHARMA**

**Department of Electrical Engineering**

**Submitted**

**in fulfilment of the requirements of the degree of Doctor of Philosophy  
to the**



**INDIAN INSTITUTE OF TECHNOLOGY DELHI**

**NOVEMBER 2021**

## **CERTIFICATE**

This is to certify that the thesis entitled, “**Design and Development of Energy Efficient Single Phase Induction Motor for Fan Applications**” being submitted by **Mr. Utkarsh Sharma** for the award of the degree of **Doctor of Philosophy** is a record of bonafide research work carried out by him in the Department of Electrical Engineering of Indian Institute of Technology Delhi.

**Mr. Utkarsh Sharma** has worked under my guidance and supervision and has fulfilled the requirements for the submission of this thesis, which to my knowledge has reached the requisite standard. The results obtained here in have not been submitted to any other University or Institute for the award of any degree.

**Date:**

**(Prof. Bhim Singh)**  
**Department of Electrical Engineering**  
**Indian Institute of Technology Delhi**  
**New Delhi-110016, India**

## ACKNOWLEDGMENTS

I feel overwhelmingly blessed to be born and raised in India. I do not find myself capable enough to thank my nation **India** and the **Government of India** for providing me with such an elite education and upbringing since my childhood. I feel overburdened to all my academic institutes, especially the **Indian Institute of Technology Delhi**, for investing a huge amount of resources in my education. I would also like to thank the **Ministry of Education** and **Science and Engineering Research Board** for sponsoring my education during these years in form of scholarships, travel grants, conference fees and other expenses. I would feel worthy enough of myself to return at least whatever I have got from my country in this life.

I would take this opportunity to share my gratitude and respect towards my supervisor **Prof. Bhim Singh** for providing his guidance and consistent supervision during the course of my Ph.D. work. I have been exceptionally fortunate to be under his benign guardianship longest time amongst his PhD students and work jointly towards the solution of one of the most challenging problems in Indian context. He has been a source of inspiration for me since the day one at IIT Delhi because of his vast knowledge, technical expertise and quick-wittedness which can ease out most serious situations. His out of the box ideas and technical suggestions have helped me during my PhD work in dealing with complex problems and situations. His constant motivation and encouragement along with corrective advices have made me a much better version of myself in past few years. He has been very kind to all of his students and has provided all the resources at his personal expense at many times. I feel blessed to be trained under his advisory and hope to take his name forward.

I wish to thank and pay my regards to **Prof. G. Bhuvaneswari**, **Prof. T. C. Kandpal**, **Prof. Ramkrishan Maheswari** and **Prof. Anandarup Das** for being supportive as well as critical of my work during research work. Their intuitive inputs have provided me with the

different perspective of looking into the research problems.

I wish to convey my sincere thanks to **Late Prof. M. L. Kothari, Prof. V. K. Jain, Prof. I. N. Kar,** and **Prof. S. M. K. Rahman** for their valuable inputs during my course work, which made the foundation for my research work.

Once again, I am grateful to IIT Delhi for providing me the research facilities. I am extremely thankful to **Sh. Srichand, Sh. Puran Singh, Mr. Amit Kumar, Mr. Jitendra, Mr. Anurag** and **Mr. Rahul** of PG Machines Lab, UG Machines Lab and Power Electronics Lab., IIT Delhi for providing me facilities and assistance during this work. I would also like to thank and indebted **Mr. Yatindra, Mr. Satish, Mr. Sandeep** and all other Electrical Engineering office staff for being supportive throughout. I am likewise thankful to those who have directly or indirectly helped me to finish my dissertation study.

I would like to thank my seniors Dr. V. Sandeep, Dr. Jeevanand, Dr. Sabharaj Arya, Dr. Arun Kumar Verma, Dr. N. K. Swami Naidu, Dr. Vashist Bist, Dr. Raj Kumar Garg, Dr. Aman Jha, Dr. Iqlakh Hussain, Dr. Sachin Devassy, Dr. Anjaneer Kumar Mishra, Dr. Radha Kushwaha Dr. Piyushkant, Dr. Sai Pranith, Dr. Nishant Kumar, Dr. Seema and Dr. Anjeet Kumar Verma for their advices and suggestions in my research work. My life in PhD would have been extremely dull without the companionship of Dr. Shailendra Dwivedi and Mr. Anshul Varshney. They have been a constant source of support and motivation for me during odd times. I would also like to thank Mr. Sreejith R. Mr. Gurmeet Singh, Ms. Subarni Pradhan, Ms. Tabish Mir, Mr. Praveen Kumar Singh, Mr. Niranjana Devela, Mr. G. K. Taneja, Mr. Girja Shankar Charan, Mr. Saurabh Mangalik, Ms. Yashi Singh for their valuable support. I would like to thank Ms. Hina Parveen and Mr. Sharankumar Shastri for treating more like elder brother than a senior and helping me out in odd times and difficult situations. I wish to convey thanks and good wishes to Mr. Amit Kumar, Mr. Vipin Kumar Singh, Mr.

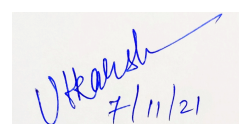
Deepak Saw for helping me out bearing with me during the joint work.

I would like to thank my friends for helping me out during all these years of hardwork with their mental and emotional support. I wish to thank especially Rajveer, Jayant, Antim, Ambuj, Jay, Nidhi ma'am, Nidhi, Ambika, Samrat Sir, Haimanti ma'am, Ankit Sir. They have become a support system for me during my PhD duration.

The hardships and sacrifices of my paternal grandfather Late Mr. Ramdas Sharma have let my family to enjoy the opportunities and comfort that I have today. Unfortunately, he left us while the duration of my PhD and is not more to see me graduating. I would like to pay my regards to my paternal grandmother Mrs. Ganga Devi Sharma for her support during all these years. I wish to thank and regards to my maternal grandparents Late Dr. Surajpal Sharma and Mrs. Om Sharma for being supportive all my life. No amount of thanks and credit is sufficient enough to reflect what my father Dr. Ashok Kumar Sharma has sacrificed to bring me to this state at expense of his own professional growth. I do not find words to thank my mother Dr. Prabha Sharma for the love, care and support that she has given me all my life. I would like to thank them for allowing me to progress on the path of research while not being bothered of my duties and Manu Sharma for being supportive and motivate me during my PhD work.

At last, I feel extremely thankful to almighty for giving such a life where I have been able to make choices that I have made and pursue the goal of higher knowledge and wisdom.

Date: 7<sup>th</sup> November 2021



Utkarsh Sharma

## ABSTRACT

Ventilating fans, particularly ceiling fans are the utmost need during summers and hot climatic conditions in India and other countries near equator. The majority of ceiling fans and exhaust fans employ permanent capacitor single phase induction motors (SPIMs). The operational number of ceiling fans and exhaust fans is enormous in countries like India, Brazil, China, USA and many more. Ceiling fans have been overlooked for efficiency throughout because of low power consumption (70 W-100 W). However, with the rising population, number of ceiling fans and exhaust fans have become exponentially high, hence their power consumption has also become enormous.

This research work deals with the analysis, design, development and testing of energy-efficient ceiling fans and exhaust fans. The radial flux SPIM based ceiling fans have a unconventional pancake type structure with two phase windings in an inner stator in very small diameter. Unlike conventional SPIMs, there are three magnetic paths of flux in the stator, each of which has to operate without saturation for minimal input power consumption. In this work, it is found that the analytical solution of the performance of the ceiling fan SPIMs is inaccurate, hence, transient mechanical finite element analysis (FEA) based solution is proposed for the performance analysis and design improvement process. The same is validated on 45 W and 50 W commercial ceiling fan motors through experimental results. The mechanical characteristics of the fan blades are identified using a torque measurement setup. A static shaft-shaft torque transducer is used for measurement of the restraining torque. Hence, the torque versus speed characteristics of the blades are identified using the curve fitting method. In this work, a simple method is proposed, which uses no load and block rotor tests along with virtual tests (from FEA) on the baseline design for identification of satisfactory performance of the ceiling fan motor for quality check of large number of motors at production level. Vari-

ous speed controllers are commercially available for controlling the speed of the ceiling fans. In this work, their impact on the performance of ceiling fan motors and power consumption is looked upon. The influence on the electrical performance and the speed control are validated with experimental tests, while the electrical performance as well as electromagnetic torque developed is analyzed using the co-simulation with FEA. The most energy-efficient ceiling fan SPIM presently consumes as low as 45 W for standard air delivery of 210 cubic meter per minute (CMM). The design of ceiling fan for 16 pole motor has been improved using the statistical methods based FEA simulations. Taguchi's orthogonal arrays are used to discretely improve the performance of the motor. A 16 pole motor design is improved to provide a service value (ratio of the air delivery in CMM and input power consumed) greater than "6". The improved design is developed, prototyped and tested for satisfactory performance for five star rating as per IS 374 and BEE five star ratings. A 14 pole configuration for radial flux ceiling fan SPIM is analyzed for improvement in the performance of motor. The design improvement along with reduction in the overall cost of the motor by using aluminium windings is proposed. Axial flux topology is explored for the use in ceiling fan motor because of higher conductor area as compared to the radial flux topologies. An analytical closed form solution is developed for the optimal design of the axial flux SPIM (AFPIM). The optimal design is verified using the transient FEA. The exhaust fan motors are the significantly higher power motors, as compared to ceiling fan motors, which are used in domestic as well as industrial environments for continuous duty. The design of a commercial exhaust fan motor is improved using a GA based computer aided design program. The optimal design results are verified using transient FEA. The exhaust fan is a type of unsymmetrical two phase machine with permanent capacitor. The transient analysis of the exhaust motor is dealt with using phase variable model and d-q axis theory. The simulated results are verified using the experimental

results on the commercial exhaust fan motor.

## सार

वेंटिलेटिंग पंखे, विशेष रूप से सीलिंग फैन की अत्यधिक आवश्यकता भारत और भूमध्य रेखा के निकट देशों में गर्मियों और गर्म जलवायु परिस्थितियों के दौरान होती है। ज्यादातर सीलिंग फैन और एजॉस्ट फैन में सिंगल फेज इंडक्शन मोटर्स (एसपीआईएम) लगाते हैं। सीलिंग फैन और एजॉस्ट फैन की परिचालन संख्या भारत, ब्राजील, चीन, अमेरिका और कई देशों में बहुत अधिक है। कम बिजली खपत (70 वाट-100 वाट) के कारण सीलिंग फैन की दक्षता की अनदेखी हमेशा से की जाती रही है। हालांकि, बढ़ती आबादी और सीलिंग फैन की संख्या के साथ, सीलिंग फैन और एजॉस्ट फैन की दक्षता में सुधार के लिए ध्यान दिया जा ना चाहिए।

इस शोध कार्य में एनर्जी एफिशिएंट सीलिंग फैन और एजॉस्ट फैन के विश्लेषण, डिजाइन, विकास और टेस्टिंग का कार्य किया गया है। रेडियल फ्लक्स (एसपीआईएम) आधारित सीलिंग पंखे की गैर-पारंपरिक पैकेजिंग संरचना में बहुत छोटे व्यास की दो फेज की वाइंडिंग स्टेटर में होती है। पारंपरिक (एसपीआईएम) के समान स्टेटर में फ्लक्स के तीन चुंबकीय पथ होते हैं, जो कि सेचुरेशन बिना न्यूनतम इनपुट बिजली खपत के लिए संचालित होते हैं। यह पाया गया है कि सीलिंग फैन (एसपीआईएम) की परफोमेन्स के लिए एनेलिटिकल सोल्युशन सही नहीं है, अतः इस कार्य में परफोमेन्स एनेलीसिस और डिजाइन सुधार प्रक्रिया के लिए ट्रान्जिएन्ट मैकेनिकल एफईए आधारित सोल्युशन प्रस्तावित है। इसे प्रायोगिक परिणामों के माध्यम से 45 वाट और 50 वाट वाणिज्यिक सीलिंग फैन मोटर्स पर मान्य किया गया है। पंखे के ब्लेड की यांत्रिक विशेषताओं को एक टॉर्क माप सेट अप का उपयोग करके पहचाना जाता है। एक स्थिर शाफ्ट-शाफ्ट टॉर्क ट्रांसड्यूसर का उपयोग निरोधक टॉर्क के मापन के लिए किया जाता है। इसलिए ब्लेड की टॉर्क बनाम गति विशेषताओं की पहचान वक्र फिटिंग विधि का उपयोग करके की जाती है।

इस कार्य में, एक सरल विधि प्रस्तावित है जो बेसलाइन डिजाइन पर नो लोड और ब्लॉक रोटर परीक्षणों का उपयोग वर्चुअल परीक्षणों के साथ-साथ सीलिंग फैन मोटर के संतोषजनक प्रदर्शन की पहचान के लिए उत्पादन स्तर पर बड़ी संख्या में मोटरों की गुणवत्ता जांच के लिए उपयोग करती है। हालांकि, सीलिंग फैन मोटर के प्रदर्शन और बिजली की खपत पर उनके प्रभाव को देखा गया है। विद्युत प्रदर्शन और गति नियंत्रण पर प्रभाव प्रयोगात्मक परीक्षणों के साथ मान्य किया गया है, जबकि विद्युत प्रदर्शन के साथ-साथ विकसित विद्युत चुंबकीय टॉर्क का विश्लेषण एफईए के साथ सह-सिमुलेशन का उपयोग करके किया गया है।

वर्तमान में सबसे अधिक एनर्जी एफिशिएंट सीलिंग फैन एसपीआईएम 45 वाट जितनी कम खपत 210 क्यूबिक मीटर प्रति मिनट (सीएमएम) के मानक वायु वितरण के लिए उपभोग करता है। 16 पोल मोटर के लिए सीलिंग फैन के डिजाइन का सुधार एफईए सिमुलेशन पर आधारित सांख्यिकीय विधियों का उपयोग करके किया गया है। टागुची ऑर्थोगोनल एरे का उपयोग मोटर के प्रदर्शन को पूरी तरह से सुधार के लिए किया जाता है। 16 पोल मोटर का सुधार "6" से अधिक सेवा मूल्य (हवा की डिलीवरी सीएमएम में और इनपुट बिजली की खपत का अनुपात) प्रदान करने के लिए किया गया है।

आईएस 374 और बीईई की पांच सितारा रेटिंग के अनुसार उन्नत डिजाइन, प्रोटोटाइप और संतोषजनक प्रदर्शन परीक्षण पांच सितारा रेटिंग के लिए विकसित किया गया है। एक 14 पोल कॉन्फ़िगरेशन रेडियल फ्लक्स सीलिंग फैन एसपीआईएम का विश्लेषण

मोटर के प्रदर्शन में सुधार के लिए किया गया है। एल्यूमीनियम वाइंडिंग का उपयोग करके मोटर की समग्र लागत में कमी के साथ-साथ डिजाइन में सुधार प्रस्तावित है। उच्च कंडक्टर क्षेत्र की वजह से एक्सियल फ्लक्स टोपोलॉजी को रेडियल फ्लक्स टोपोलॉजी की तुलना में सीलिंग फैन मोटर में उपयोग के लिए पता लगाया गया है। एक्सियल फ्लक्स एसपीआईएम (एफपीआईएम) के ऑप्टीमल डिजाइन के लिए एक एनेलिटिकल क्लोज्ड फॉर्म सोल्युशन विकसित किया गया है। ऑप्टीमल डिजाइन का सत्यापन ट्रान्जिएन्ट एफईए का उपयोग करके किया गया है। एग्जॉस्ट फैन मोटर्स काफी उच्च शक्ति वाली मोटर्स हैं जिनका उपयोग घरेलू और औद्योगिक वातावरण में निरंतर ड्यूटी के लिए किया जाता है। एक व्यावसायिक एग्जॉस्ट फैन मोटर्स के डिजाइन में सुधार जीए आधारित कंप्यूटर एडेड डिजाइन प्रोग्राम का उपयोग करके किया गया है। ऑप्टीमल डिजाइन का सत्यापन ट्रान्जिएन्ट एफईए का उपयोग करके किया गया है। एग्जॉस्ट फैन एक प्रकार की असममित दो फेस मशीन है जिसमें स्थायी संधारित्र होता है। एग्जॉस्ट मोटर का ट्रान्जिएन्ट एनेलीसिस फेस वेरीएबल मॉडल और डी-क्यू सिद्धांत का उपयोग करके किया गया है। व्यावसायिक एग्जॉस्ट फैन मोटर के सिमुलेटेड परिणामों को प्रयोगात्मक परिणामों से सत्यापित किया गया है।

# TABLE OF CONTENTS

	<b>Page</b>
Certificate	i
Acknowledgments	ii
Abstract	v
Hindi Abstract	viii
List of Figures	xvi
List of Tables	xxvii
List of Abbreviations	xxix
List of Symbols	xxxi
<b>CHAPTER - I INTRODUCTION</b>	<b>1-17</b>
1.1 General	1
1.2 Impact of Energy Consumption of Ceiling Fans in World and India	4
1.3 State of Art of Fans	6
1.3.1 Single Phase Induction Motor Based Ceiling Fans	7
1.3.2 Permanent Magnet Brushless DC Motor Fans	8
1.3.3 Permanent Magnet Synchronous Motor Ceiling Fans	8
1.3.4 Switched Reluctance Motor Ceiling Fans	9
1.3.5 Exhaust Fan Motors	10
1.4 Standards and Regulations for Fans Over World	11
1.4.1 Standards and Regulations In India	11
1.4.2 Standards and Regulations Across World	12
1.5 Classification of Ceiling Fans in Indian Market	13
1.6 Design Aspects of Ceiling Fan Motors	14
1.6.1 Mechanical Design Aspects	14
1.6.2 Electrical Design Aspects	15
1.6.3 Blade Design Aspects	15
1.7 Objectives and Scope of Work	16
1.8 Outline of Chapters	17
<b>CHAPTER - II LITERATURE REVIEW</b>	<b>21-36</b>
2.1 General	21
2.2 Literature Survey	22
2.2.1 Single Phase Induction Motors	22
2.2.1.1 Theory and Operation of SPIMs	24
2.2.1.2 Speed Control of the SPIMs	25
2.2.2 Outer Rotor Single Phase Induction Motor Ceiling Fans	27
2.2.3 Axial Flux Single Phase Induction Motor Ceiling Fans	28

2.2.4	Permanent Magnet Brushless DC / Synchronous Motor Ceiling Fans	29
2.2.5	Switched Reluctance Motor Ceiling Fans	30
2.2.6	Impact of Blades on Performance of Ceiling Fans	32
2.2.7	Robust Design Methodologies and Optimization Techniques	33
2.3	Identified Research Areas	34
2.4	Conclusions	36
 <b>CHAPTER - III PERFORMANCE EVALUATION OF CAPACITOR RUN SINGLE PHASE INDUCTION MOTOR CEILING FANS</b>		 37-78
3.1	General	37
3.2	Performance Analysis of Energy Efficient Single Phase Induction Motor Ceiling Fans	38
3.2.1	Measurement of Lumped Parameters of Ceiling Fans Using No Load and Blocked Rotor Tests	39
3.2.2	Performance Analysis From Equivalent Circuit Analysis	40
3.2.3	Comparison of Experimental Performance with Analytical Performance Estimated From Lumped Parameters	41
3.2.4	Experimental Setup for Measurement of Output Power and Torque of Domestic Ceiling Fans	46
3.2.4.1	Specifications of Torque Transducer	48
3.2.4.2	Calibration of Torque Transducer	49
3.2.4.3	Mechanical Assembly for Torque Measurement	51
3.2.4.4	Characteristics of the Energy-Efficient Ceiling Fan Blades	51
3.2.5	Transient Finite Element Analysis for Performance Evaluation of Single Phase Induction Motor for Ceiling Fan	53
3.2.5.1	Design Data of Existing Energy-Efficient Ceiling Fan SPIM	55
3.2.5.2	Development of Finite Element Based Model	56
3.2.5.3	Validation of Experimental Performance of Energy Efficient Ceiling Fan SPIM	57
3.3	Parametric Analysis of Design Parameters on Performance of Energy-Efficient Ceiling Motor	61
3.3.1	Impact of Airgap Variation on Performance of Ceiling Fan SPIM	61
3.3.2	Impact of Main Winding Turns on Performance of Ceiling Fan SPIM	62
3.3.3	Impact of Auxiliary Winding Turns on Performance of Ceiling Fan SPIM	64
3.3.4	Impact of Stack Height on Performance of Ceiling Fan SPIM	65
3.3.5	Impact of Capacitor Value Variation on Performance of Ceiling Fan SPIM	67
3.4	Design Based Approach for Mass Testing of Ceiling Fan SPIMs	68
3.4.1	Influence of Airgap Variation From Testing Point of View	70
3.4.2	Influence of Leakage Reactance From Testing Point of View	71

3.4.3	Proposed Methodology	72
3.4.3.1	Bench-Marking of Blades	74
3.4.3.2	Virtual Tests and Simulations	74
3.4.3.3	Tests of Sample Motor	74
3.4.4	Results and Discussion	75
3.4.4.1	Actual Testing of Sample Motors	75
3.4.4.2	Determination of Quality of Sample Motors	77
3.5	Conclusions	78

**CHAPTER - IV PERFORMANCE ANALYSIS OF SPEED CONTROLLERS  
FOR SPIM CEILING FAN** 80-114

4.1	General	80
4.2	Types of Speed Controllers for Ceiling Fans	80
4.3	Comparative Analysis of Various Speed Controllers With Co-Simulation Based Finite Element Analysis and Experimental Tests	82
4.4	Results and Discussion	84
4.4.1	Performance Analysis of Resistive Based Controller For Ceiling Fan	84
4.4.1.1	Experimental Testing of Resistive Based Controller With Ceil- ing Fan	86
4.4.1.2	FEA Based Co-Simulation of Resistive Based Controller With Ceiling Fan	88
4.4.2	Performance Analysis of Capacitive Based Controller With Ceiling Fan	95
4.4.2.1	Experimental Testing of Capacitive Based Controller With Ceil- ing Fan	95
4.4.2.2	FEA Based Co-Simulation of Capacitive Based Controller With Ceiling Fan	97
4.4.3	Performance Analysis of TRIAC based Controller with ceiling fan	101
4.4.3.1	Experimental Testing of TRIAC based Controller with ceiling fan	103
4.4.3.2	FEA based Co-Simulation of TRIAC Based Controller With Ceiling Fan	110
4.5	Conclusions	114

**CHAPTER - V DESIGN AND DEVELOPMENT OF LOW SPEED SINGLE  
PHASE INDUCTION MOTOR CEILING FAN** 116-158

5.1	General	116
5.2	Design for Performance Improvement of Single Phase Induction Motor for Ceiling Fan	116
5.2.1	Design of Energy Efficient SPIM Ceiling Fan Motor for Higher Efficacy	118

5.2.1.1	Design Problem Formulation	120
5.2.1.2	Taguchi's Orthogonal Array [172]	120
5.2.1.3	Analysis of Average For Each Parameter	121
5.2.1.4	Simulation Based Design of Energy Efficient SPIM Ceiling Fan Motor for Higher Efficacy	122
5.2.2	Design of Single Phase Induction Motor for Ceiling Fan for Higher Efficacy and Standard Air Delivery	129
5.2.2.1	Design Problem Formulation	130
5.2.2.2	Simulation Based Design of Energy Efficient Ceiling Fan Motor for Higher Efficacy and Standard Air Delivery	131
5.2.3	Design of Single Phase Induction Motor for 5 Star Rated Ceiling Fan as Per IS: 374 and BEE	133
5.2.3.1	Design Problem Formulation	133
5.2.3.1.1	Width of Main and Auxiliary Windings Teeth	133
5.2.3.1.2	Consideration of Fill Factor	134
5.2.3.1.3	Starting Torque of Motor with Higher Motor Diameter	135
5.2.3.2	Simulation Based Design of Energy Efficient Ceiling Fan Single Phase Induction Motor as Per IS: 374 and BEE	135
5.3	Development of Prototypes for SPIM based Ceiling Fans	139
5.3.1	Prototyping of First Design	139
5.3.2	Prototyping of Second Design	140
5.3.3	Prototyping of Third Design	141
5.4	Results and Discussion	143
5.4.1	Simulated and Experimental Results of Energy Efficient SPIM Motor with Higher Efficacy	143
5.4.1.1	Simulation Results	143
5.4.1.2	Experimental Results	144
5.4.2	Simulated and Experimental Results of Energy Efficient SPIM for Lower Input Power and Standard Air Delivery	147
5.4.2.1	Simulation Results	147
5.4.2.2	Experimental Results	148
5.4.3	Simulated and Experimental Results of Five Star Rated Ceiling Fan as Per IS: 374 and Bureau of Energy Efficiency	153
5.4.3.1	Simulation Results	153
5.4.3.2	Experimental Results	156
5.5	Conclusions	158

<b>CHAPTER - VI</b>	<b>DESIGN AND DEVELOPMENT OF HIGH SPEED SINGLE PHASE INDUCTION MOTOR CEILING FAN</b>	<b>160-180</b>
6.1	General	160
6.2	Design Problem Formulation	161
6.2.1	Design Considerations for High Speed Ceiling Fan Single Phase Induction Motor with Higher Diameter	163
6.2.1.1	Number of Poles of Motor	163
6.2.1.2	Selection of Outer Diameter of Motor	163
6.2.1.3	Design of Blade For Selected Number of Poles	164
6.2.2	Modifications in Stator and Rotor Laminations	164
6.2.3	Comparison of Properties of Copper and Aluminium For Ceiling Fan Motor Winding	166
6.2.3.1	Difference in Resistivity of Aluminium and Copper	167
6.2.3.2	Difference in Thermal Conductivity of Aluminium and Copper	167
6.2.3.3	Difference in Mass of Windings with Aluminium and Copper	168
6.2.3.4	Difference in Cost of Windings with Aluminium and Copper	168
6.3	Design of Energy-Efficient Ceiling Fan SPIM With Higher Diameter	169
6.4	Results and Discussion	172
6.4.1	Performance Analysis of Energy-Efficient Ceiling Fan SPIM with 200 mm OD	173
6.4.2	Performance Analysis of Energy-Efficient Ceiling Fan SPIM with 220 mm OD	175
6.4.3	Cost Analysis and Feasibility Analysis of Energy Efficient Design	178
6.5	Conclusions	180
<b>CHAPTER - VII</b>	<b>DESIGN AND DEVELOPMENT OF AXIAL FLUX SINGLE PHASE INDUCTION MOTOR FOR CEILING FAN</b>	<b>182-201</b>
7.1	General	182
7.2	Design Problem Formulation	183
7.2.1	Design Considerations for Axial Flux Single Phase Induction Motor For Ceiling Fan	184
7.2.1.1	Number of Poles in Motor	184
7.2.1.2	Selection of Outer Diameter and Sizing of Motor	184
7.2.1.3	Design of Blade for Selected Number of Poles	185
7.3	Analytical Design Formulation for Axial Flux Single Phase Induction Motor Based Ceiling Fan	185
7.3.1	Sizing of Motor	185
7.3.2	Determination of Equivalent Circuit Parameters	188
7.3.2.1	Calculation of Stator and Rotor Winding Resistances	188

7.3.2.2	Calculation of Magnetizing Inductance	189
7.3.2.3	Calculation of Stator and Rotor Leakage Inductances	189
7.3.3	Saturation and Core Losses Calculations	191
7.3.4	Performance Analysis of AFSPIM Motor	192
7.4	Design Optimization For Axial Flux Single Phase Induction Motor For Ceiling Fan	192
7.4.1	Selection of Design Variables for Optimization of Axial Flux Ceiling Fan Single Phase Induction Motor	193
7.4.2	Range of Design Variables for Optimization	195
7.4.3	Design Optimization Using GA	195
7.5	Validation of Optimal Design With Finite Element Analysis (FEA)	196
7.6	Results and Discussion	198
7.6.1	Simulated Performance of the Optimal Design	198
7.6.2	Cost Analysis and Weight of Optimal Design	200
7.7	Conclusions	201

**CHAPTER - VIII DESIGN AND DEVELOPMENT OF ENERGY EFFICIENT EXHAUST FAN INDUCTION MOTOR** 203-233

8.1	General	203
8.2	Existing Exhaust Fan Motor Design and Performance Analysis	204
8.3	Transient Model for Performance Estimation of Permanent Capacitor Single Phase Induction Motors	206
8.3.1	Analysis of Exhaust Fan Single Phase Induction Motor Using Phase variables	208
8.3.2	Analysis of Exhaust Fan Single Phase Induction Motor Using d-q Axis Variables	212
8.4	Design Optimization Problem Formulation	215
8.4.1	Selection of Materials	218
8.4.2	Design of Stator	218
8.4.3	Design of Rotor	218
8.4.4	Analytical Design Formulation for Exhaust Fan Single Phase Induction Motor	219
8.4.5	Determination of Equivalent Circuit Parameters	221
8.4.5.1	Calculation of Stator and Rotor Winding Resistances	221
8.4.5.2	Calculation of Magnetizing Inductance	222
8.4.5.3	Calculation of Stator and Rotor Leakage Inductances	222
8.4.6	Saturation and Core Losses Calculations	224
8.5	Optimization of Exhaust Fan Single Phase Induction Motor	225

8.5.1	Selection of Design Variables for Design of Energy-Efficient Exhaust Fan Single Phase Induction Motor	228
8.5.2	Range of Design Variables for Optimization	228
8.6	Performance Analysis of Optimal Design Using Finite Element Analysis	229
8.7	Results and Discussion	229
8.7.1	Performance of Optimal Design	230
8.7.2	Validation of Optimal Design Using FEA	231
8.7.3	Cost Analysis and Weight of Energy Efficient Design	232
8.8	Conclusions	233
<b>CHAPTER - IX MAIN CONCLUSIONS AND SUGGESTIONS FOR FURTHER WORK</b>		234-239
9.1	General	234
9.2	Main Conclusions	234
9.3	Suggestion for Further Work	239
<b>REFERENCES</b>		241
<b>APPENDICES</b>		253
<b>LIST OF PUBLICATIONS</b>		272
<b>BIO-DATA</b>		274

## LIST OF FIGURES

Fig. 1.1	Consumption by household appliances and plug loads by region in sustainable development scenario in (TWh)	1
Fig. 1.2	Population without access to an AC, including potential access in a cooling for all scenario, 1990-2100	2
Fig. 1.3	(a) Stator of a commercial ceiling fan SPIM, (b) Rotor of a commercial ceiling fan SPIM	8
Fig. 1.4	(a) A commercial BLDC ceiling fan motor, (b) Power converter of a commercial BLDC ceiling fan motor [21]	9
Fig. 1.5	(a) Two phase SRM ceiling fan motor cross-section, (b) Power controller for SRM ceiling fan motor [24]	10
Fig. 3.1	(a) Cross-sectional view of the ceiling fan SPIM, (b) Flux paths in a ceiling fan SPIM	38
Fig. 3.2	(a) Equivalent circuit at no load and block rotor from [73,165], (b) Equivalent circuit at no load and block rotor from [79]	40
Fig. 3.3	(a) Equivalent circuit at rated condition from [73, 165], (b) Equivalent circuit at rated condition from [79]	41
Fig. 3.4	Test results on 16 pole motor (a) Rated speed test with $U_{rms1}$ as supply voltage, (b) Rated speed test with $U_{rms1}$ as auxiliary winding voltage, (c) No load test on main winding, (d) Block rotor test on main winding, (e) No load test on auxiliary winding, (f) Block rotor test on auxiliary winding	44
Fig. 3.5	Test results on 14 pole motor (a) Rated speed test with $U_{rms1}$ as supply voltage, (b) Rated speed test with $U_{rms1}$ as auxiliary winding voltage, (c) No load test on main winding, (d) Block rotor test on main winding, (e) No load test on auxiliary winding, (f) Block rotor test on auxiliary winding	45
Fig. 3.6	16 Pole motor comparison of performance from equivalent circuit methods with experimental performance (a) Variation of speed with voltage, (b) Comparison of supply current with voltage, (c) Comparison of Input power with voltage (d) Comparison of power factor with voltage	47
Fig. 3.7	14 Pole motor comparison of performance from equivalent circuit methods with experimental performance (a) Variation of speed with voltage, (b) Comparison of supply current with voltage, (c) Comparison of Input power with voltage (d) Comparison of power factor with voltage	47
Fig. 3.8	TTS- Mini Transducer calibration setup	50

Fig. 3.9	(a) Torque transducer TTS-Mini, (b) Arrangement of torque transducer in between two down-rods of ceiling fan, (c) Testbench for measurement of torque of ceiling fan	52
Fig. 3.10	Torque vs Speed characteristics of tested blades	53
Fig. 3.11	FEA models of energy-efficient ceiling fan SPIMs (a) 45 W motor model with applied mesh settings, (b) 50 W motor model with applied mesh settings	57
Fig. 3.12	Flux density map of steel part in 16 pole motor at (a) Instant when flux is concentrated around main winding slot, (b) Instant when flux is concentrated around auxiliary winding slot, (c) Instant when flux is concentrated around teeth bridge between main winding slot and auxiliary winding slot	59
Fig. 3.13	Flux density map of steel part in 14 pole motor (a) Instant when flux is concentrated around main winding slot, (b) Instant when flux is concentrated around auxiliary winding slot, (c) Instant when flux is concentrated around teeth bridge between main winding slot and auxiliary winding slot	59
Fig. 3.14	Performance of 16 pole motor from FEA at rated load (a) Torque versus speed characteristics of motor and blade, (b) Supply and winding currents at steady state, (c) Airgap flux density distribution in space, (d) Harmonic spectrum of airgap flux density	60
Fig. 3.15	Performance of the 14 pole motor from FEA at rated load (a) Torque versus speed characteristics of the motor and blade, (b) Supply and winding currents at steady state, (c) Airgap flux density distribution in space, (d) Harmonic spectrum of airgap flux density	61
Fig. 3.16	Effect of airgap variation (a) Speed, (b) Motor efficiency and output power, (c) Supply and winding currents at rated load, (d) Supply and winding currents at no load, (e) Power factor at rated load, (f) Motor losses at rated load	63
Fig. 3.17	Effect of main winding turns variation (a) Speed, (b) Motor efficiency and output power, (c) Supply and winding currents at rated load, (d) Supply and winding currents at no load, (e) Power factor at rated load, (f) Motor losses at rated load	64
Fig. 3.18	Effect of auxiliary winding turns Variation, (a) Speed, (b) Motor efficiency and output power, (c) Supply and winding currents at rated load, (d) Supply and winding currents at no load, (e) Power factor at rated load, (f) Motor losses at rated load	66

Fig. 3.19	Effect of Stack Height Variation, (a) Speed, (b) Motor efficiency and output power, (c) Supply and winding currents at rated load, (d) Supply and winding currents at no load, (e) Power factor at rated load, (f) Motor losses at rated load	67
Fig. 3.20	Effect of Capacitor Variation, (a) Speed, (b) Motor efficiency and output power, (c) Supply and winding currents at rated load, (d) Supply and winding currents at no load, (e) Power factor at rated load, (f) Motor losses at rated load	69
Fig. 3.21	Impact of airgap variation on the performance of ceiling fan SPIM (a) Output and Input Power, (b) Torque developed by the motor	71
Fig. 3.22	Impact of leakage reactance variation on the performance of ceiling fan SPIM (a) Output and Input Power, (b) Torque developed by the motor	72
Fig. 3.23	Proposed testing method for SPIM for ceiling fans	73
Fig. 3.24	Experimental test on Sample I (a) No load test, (b) Block rotor test, (c) Rated speed test	76
Fig. 3.25	Experimental test on Sample II (a) No load test, (b) Block rotor test, (c) Rated speed test	76
Fig. 3.26	Experimental test on Sample III (a) No load test, (b) Block rotor test, (c) Rated speed test	77
Fig. 4.1	Resistive speed controller for ceiling fan	81
Fig. 4.2	TRIAC based speed controller for ceiling fan	82
Fig. 4.3	Capacitive speed controller for ceiling fan	83
Fig. 4.4	Simplorer based co-simulation of the ceiling fan SPIM with speed controller (a) Resistive Controller, (b) Capacitive Controller, (c) TRIAC Controller	85
Fig. 4.5	Comparison of performance of a 16 pole ceiling fan with resistive speed controller (a) Speed versus input voltage, (b) Supply current versus input voltage, (c) Supply power factor versus input voltage, (d) Supply power versus input voltage	87
Fig. 4.6	Comparison of performance of a 14 pole ceiling fan with resistive speed controller (a) Speed versus input voltage, (b) Supply current versus input voltage, (c) Supply power factor versus input voltage, (d) Supply power versus input voltage	87

Fig. 4.7	Performance parameters of a 16 pole motor with resistive controller at lowest motor voltage setting (a) Motor voltage, motor current, motor input power and motor power factor, (b) Harmonic spectrum of the motor current and motor input voltage, (c) Supply voltage, supply current, supply input power and supply power factor, (d) Harmonic spectrum of the supply current and supply input voltage, (e) Wave-forms of supply supply voltage, main winding voltage, auxiliary winding voltage and capacitor voltage, (f) Wave-forms of supply voltage, supply current, main winding current and auxiliary winding current	89
Fig. 4.8	Performance parameters of a 14 pole motor with resistive controller at lowest motor voltage setting (a) Motor voltage, motor current, motor input power and motor power factor, (b) Harmonic spectrum of the motor current and motor input voltage, (c) Supply voltage, supply current, supply input power and supply power factor, (d) Harmonic spectrum of the supply current and supply input voltage, (e) Wave-forms of supply supply voltage, main winding voltage, auxiliary winding voltage and capacitor voltage, (f) Wave-forms of supply voltage, supply current, main winding current and auxiliary winding current	90
Fig. 4.9	Simulated performance of ceiling fan motors at rated voltage (a) Simulated electromagnetic torque of a 16 pole motor, (b) Simulated supply voltage and motor current for 16 pole motor, (c) Simulated electromagnetic torque of 14 pole motor, (d) Simulated supply voltage and motor current for 14 pole motor	91
Fig. 4.10	Simulated waveforms of electromagnetic torque developed in a 16 pole motor with resistive controller at (a) 161 V, (b) 181 V, (c), 196 V, (d) 210 V	93
Fig. 4.11	Simulated waveforms of electromagnetic torque developed in 14 pole motor at (a) 152V, (b) 172V, (c) 189 V, (d) 206 V	94
Fig. 4.12	Comparison of performance of a 16 pole ceiling fan with capacitive speed controller (a) Speed versus input voltage, (b) Supply current versus input voltage, (c) Supply power factor versus input voltage, (d) Supply power versus input voltage	96
Fig. 4.13	Comparison of performance of a 14 pole ceiling fan with capacitive speed controller (a) Speed versus input voltage, (b) Supply current versus input voltage, (c) Supply power factor versus input voltage, (d) Supply power versus input voltage	96

Fig. 4.14	Performance parameters of a 16 pole motor with capacitive controller at lowest motor voltage setting (a) Motor voltage, motor current, motor input power and motor power factor, (b) Harmonic spectrum of the motor current and motor input voltage, (c) Supply voltage, supply current, supply input power and supply power factor, (d) Harmonic spectrum of the supply current and supply input voltage, (e) Wave-forms of supply supply voltage, main winding voltage, auxiliary winding voltage and capacitor voltage, (f) Wave-forms of supply voltage, supply current, main winding current and auxiliary winding current	98
Fig. 4.15	Performance parameters of a 14 pole motor with capacitive controller at lowest motor voltage setting (a) Motor voltage, motor current, motor input power and motor power factor, (b) Harmonic spectrum of the motor current and motor input voltage, (c) Supply voltage, supply current, supply input power and supply power factor, (d) Harmonic spectrum of the supply current and supply input voltage, (e) Wave-forms of supply supply voltage, main winding voltage, auxiliary winding voltage and capacitor voltage, (f) Wave-forms of supply voltage, supply current, main winding current and auxiliary winding current	99
Fig. 4.16	Simulated waveforms of electromagnetic torque developed in a 16 pole motor with capacitive controller at (a) 151 V, (b) 181 V, (c), 208 V	102
Fig. 4.17	Simulated waveforms of electromagnetic torque developed in a 14 pole motor with capacitive controller at (a) 128 V, (b) 158V, (c), 186 V	102
Fig. 4.18	Comparison of performance of a 16 pole ceiling fan with TRIAC based speed controller (a) Speed versus input voltage, (b) Supply current versus input voltage, (c) Supply power factor versus input voltage, (d) Supply power versus input voltage	104
Fig. 4.19	Comparison of performance of a 14 pole ceiling fan with TRIAC based speed controller (a) Speed versus input voltage, (b) Supply current versus input voltage, (c) Supply power factor versus input voltage, (d) Supply power versus input voltage	104
Fig. 4.20	Performance parameters of a 16 pole motor with TRIAC controller at lowest motor voltage setting (a) Motor voltage, motor current, motor input power and motor power factor, (b) Harmonic spectrum of the motor current and motor input voltage, (c) Supply voltage, supply current, supply input power and supply power factor, (d) Harmonic spectrum of the supply current and supply input voltage, (e) Wave-forms of supply supply voltage, main winding voltage, auxiliary winding voltage and capacitor voltage, (f) Wave-forms of supply voltage, supply current, main winding current and auxiliary winding current	106

Fig. 4.21	Performance parameters of a 14 pole motor with TRIAC controller at lowest motor voltage setting (a) Motor voltage, motor current, motor input power and motor power factor, (b) Harmonic spectrum of the motor current and motor input voltage, (c) Supply voltage, supply current, supply input power and supply power factor, (d) Harmonic spectrum of the supply current and supply input voltage, (e) Wave-forms of supply supply voltage, main winding voltage, auxiliary winding voltage and capacitor voltage, (f) Wave-forms of supply voltage, supply current, main winding current and auxiliary winding current	107
Fig. 4.22	Comparison of performance of a 16 pole ceiling fan with TRIAC speed controller with resistive speed controller (a) Speed versus input voltage, (b) Supply current versus input voltage, (c) Supply power factor versus input voltage, (d) Supply power versus input voltage	108
Fig. 4.23	Comparison of performance of a 14 pole ceiling fan with TRIAC speed controller with resistive speed controller (a) Speed versus input voltage, (b) Supply current versus input voltage, (c) Supply power factor versus input voltage, (d) Supply power versus input voltage	109
Fig. 4.24	Comparison of performance of a 16 pole ceiling fan with TRIAC speed controller with capacitive speed controller (a) Speed versus input voltage, (b) Supply current versus input voltage, (c) Supply power factor versus input voltage, (d) Supply power versus input voltage	110
Fig. 4.25	Comparison of performance of a 14 pole ceiling fan with TRIAC speed controller with capacitive speed controller (a) Speed versus input voltage, (b) Supply current versus input voltage, (c) Supply power factor versus input voltage, (d) Supply power versus input voltage	111
Fig. 4.26	Simulated waveforms of electromagnetic torque developed in a 16 pole motor with TRIAC controller at (a) 173 V, (b) 193 V, (c), 204 V, (d) 222 V	112
Fig. 4.27	Simulated waveforms of electromagnetic torque developed in a 14 pole motor with TRIAC controller at (a) 174 V, (b) 195 V, (c), 211 V, (d) 221 V	113
Fig. 5.1	(a) Airgap flux density in 16 Pole SPIM under rated excitation (Multi Slice 2D FEA), (b) Air gap MMF in a 16 Pole ceiling fan SPIM	118
Fig. 5.2	Details of commercially available ceiling fan SPIM (a) Commercial ceiling fan stator, (b) Rated performance of motor	119
Fig. 5.3	Flux density plot of existing ceiling fan motor at rated loading	119
Fig. 5.4	Stages of formation of Orthogonal arrays of runs	122
Fig. 5.5	Analysis of averages plot for (a) First L18 OA, (b) Second L18 OA	126
Fig. 5.6	Analysis of averages plot for (a) L4 OA, (b) L8 OA	128

Fig. 5.7	(a) Comparison of the old and new stator lamination (b) Comparison of the old rotor slot with new rotor slot	129
Fig. 5.8	Scatter plot showing feasible designs, (a) Input Power versus Speed versus Torque, (b) Losses versus Mass versus Torque, (c), Speed versus Output Power versus Efficiency, (d) Power Factor versus Torque versus Speed	131
Fig. 5.9	Flowchart for overall design of 5 star rated SPIM ceiling fan	137
Fig. 5.10	Scatter plot showing feasible designs, (a) Input Power versus Speed versus Torque, (b) Losses versus Mass versus Torque, (c), Speed versus Output Power versus Efficiency, (d) Power Factor versus Torque versus Speed	138
Fig. 5.11	(a) Comparison of the old and new stator lamination (b) Comparison of the old rotor slot with new rotor slot	138
Fig. 5.12	Developmental photographs of first prototype (a) Stator with both windings, (b) Single steel lamination, (c) Aluminium die-casted rotor.	140
Fig. 5.13	Developmental photographs of second prototype (a) Stator with both windings wound, (b) Aluminium die-casted rotor	141
Fig. 5.14	Developmental photographs of third prototype (a) Stator with both windings wound, (b) Aluminium die-casted rotor, (c) Modified blade with new motor body, (d) Comparison of existing blade with modified blade	142
Fig. 5.15	Simulated FEA performance of improved design (a) Flux density in stator and rotor steel part, (b) Flux lines in the motor magnetic circuit, (c) Air gap radial flux density plot with respect to mechanical angle of optimal design, (d) Comparison of harmonic spectrum of air gap flux density of optimal design with existing motor	144
Fig. 5.16	Test results of first prototype (a) No load test results, (b) Block rotor test results, (c) Test result at rated speed, (d), $V_{supply}$ , $I_{supply}$ , $I_{main}$ , $I_{aux}$ , (e) $V_s$ , $V_{main}$ , $V_{aux}$ , $V_C$	146
Fig. 5.17	Test results for comparison of prototype with existing fan motor (a) Speed with respect to input voltage (b) Supply current with respect to input voltage (c) Power factor with respect to input voltage (d) Power with respect to input voltage	147
Fig. 5.18	Test results for comparison of prototype with existing fan motor with TRIAC controller (a) Speed with respect to TRIAC voltage (b) Supply current with respect to TRIAC voltage (c) Power factor with respect to TRIAC voltage (d) Power with respect to TRIAC voltage	148

Fig. 5.19	Simulated FEA performance of improved design (a) Flux density in stator and rotor steel part, (b) Flux lines in the motor magnetic circuit, (c) Air gap radial flux density plot with respect to mechanical angle of optimal design, (d) Comparison of harmonic spectrum of air gap flux density of optimal design with existing motor	149
Fig. 5.20	Test results of the prototype (higher wire gauge) (a) No load test results, (b) Block rotor test results, (c) Test result at rated speed, (d), $V_{supply}$ , $I_{supply}$ , $I_{main}$ , $I_{aux}$ (e) $V_s$ , $V_{main}$ , $V_{aux}$ , $V_C$	152
Fig. 5.21	Test results of the prototype (lower turns)(a) No load test results, (b) Block rotor test results, (c) Test result at rated speed, (d), $V_{supply}$ , $I_{supply}$ , $I_{main}$ , $I_{aux}$ (e) $V_s$ , $V_{main}$ , $V_{aux}$ , $V_C$	152
Fig. 5.22	Test results for comparison of prototype with existing fan motor (a) Speed with respect to input voltage (b) Supply current with respect to input voltage (c) Power factor with respect to input voltage (d) Power with respect to input voltage	153
Fig. 5.23	Test results for comparison of prototype with existing fan motor with TRIAC controller (a) Speed with respect to TRIAC voltage (b) Supply current with respect to TRIAC voltage (c) Power factor with respect to TRIAC voltage (d) Power with respect to TRIAC voltage	154
Fig. 5.24	Simulated FEA performance of third design (a) Flux density in the stator and rotor steel part, (b) Flux lines in the motor magnetic circuit, (c) Air gap radial flux density plot with respect to mechanical angle of optimal design, (d) Comparison of harmonic spectrum of the air gap flux density of optimal design with existing motor	155
Fig. 5.25	Test results of prototype (lower turns) (a) No load test results, (b) Block rotor test results, (c) Test result at rated speed, (d), $V_{supply}$ , $I_{supply}$ , $I_{main}$ , $I_{aux}$ (e) $V_s$ , $V_{main}$ , $V_{aux}$ , $V_C$	157
Fig. 5.26	Test results for comparison of prototype with existing fan motor (a) Speed with respect to input voltage (b) Supply current with respect to input voltage (c) Power factor with respect to input voltage (d) Power with respect to input voltage	158
Fig. 5.27	Test results for comparison of prototype with existing fan motor with TRIAC controller (a) Speed with respect to TRIAC voltage (b) Supply current with respect to TRIAC voltage (c) Power factor with respect to TRIAC voltage (d) Power with respect to TRIAC voltage	159
Fig. 6.1	Flux density plot of reference SPIM motor at rated loading, Left: Concentrated in auxiliary winding teeth, Right: Concentrated in main winding teeth	162

Fig. 6.2	Comparison of 14 pole higher diameter stator lamination with existing lamination (a) existing motor with 152.4 mm diameter (b) 200 mm outer diameter (c) 220 mm outer diameter	166
Fig. 6.3	Scatter plot showing feasible designs with 200 mm OD, (a) Input Power versus Speed versus Torque, (b) Losses versus Mass versus Torque, (c), Speed versus Output Power versus Efficiency, (d) Power Factor versus Torque versus Speed	170
Fig. 6.4	Scatter plot showing feasible designs with 220 mm OD, (a) Input Power versus Speed versus Torque, (b) Losses versus Mass versus Torque, (c), Speed versus Output Power versus Efficiency, (d) Power Factor versus Torque versus Speed	172
Fig. 6.5	Plots showing performance of the 200 mm OD design with copper winding (a), Torque versus speed characteristics of the motor and load (b), Steady state winding currents and supply current (c), Airgap radial flux density (d) Harmonic spectrum of the airgap flux density	175
Fig. 6.6	Plots showing performance of 200 mm OD design with aluminium winding (a), Torque versus speed characteristics of motor and load (b), Steady state winding currents and supply current (c), Airgap radial flux density (d) Harmonic spectrum of airgap flux density	176
Fig. 6.7	Flux density distribution of at rated operating condition in 200 mm OD (concentration around left: main winding slot, right: auxiliary winding slot) (a) Copper winding motor, 6.7(b) Aluminium winding motor	176
Fig. 6.8	Plots showing performance of 220 mm OD design with copper winding (a), Torque versus speed characteristics of motor and load (b), Steady state winding currents and supply current (c), Airgap radial flux density (d) Harmonic spectrum of airgap flux density	178
Fig. 6.9	Plots showing performance of 220 mm OD design with aluminium winding (a), Torque versus speed characteristics of motor and load (b), Steady state winding currents and supply current (c), Airgap radial flux density (d) Harmonic spectrum of airgap flux density	179
Fig. 6.10	Flux density distribution of at rated operating condition in 220 mm OD (concentration around left: main winding slot, right: auxiliary winding slot) (a) Copper winding motor, 6.10(b) Aluminium winding motor	179
Fig. 7.1	Construction of a typical permanent capacitor axial flux single phase induction motor	186
Fig. 7.2	Slot profiles for (a) Stator Slot and (b) Rotor Slot	193
Fig. 7.3	Flowchart for implementation of GA based optimization of AFSPIM	197
Fig. 7.4	Reduced model of AFPIM with meshing	198

Fig. 7.5	Simulated performance of optimal design (a) Output power versus slip, (b) Supply current versus slip, (c) Electromagnetic torque and load torque versus slip, (d) Power factor versus slip	200
Fig. 7.6	Performance of AFSPIM at rated condition from 3D FEA (a) Torque versus speed characteristics of motor and load, (b) Supply currents and winding currents, (c) Flux density magnitude in steel parts, (d) Direction of flux path in steel parts	201
Fig. 8.1	Stator and rotor of existing exhaust fan motor	204
Fig. 8.2	Test results of existing exhaust fan (a)-(b) Rated performance, (c)-(d) No load performance, (e) Waveforms of the supply voltage ( $V_{supply}$ ), main winding voltage ( $V_{supply}$ ), auxiliary winding voltage ( $V_{aux}$ ) and capacitor voltage ( $V_C$ ) at rated condition, (f) Waveforms of the supply voltage ( $V_{supply}$ ), supply current ( $I_{supply}$ ), main winding current ( $I_{main}$ ) and auxiliary winding current ( $I_{aux}$ ) at rated condition	205
Fig. 8.3	No load and block rotor tests on main and auxiliary winding for calculation of equivalent circuit parameters (a) No load test on main winding, (b) Block rotor test on main winding, (c) No load test on auxiliary winding, (d) Block rotor test on auxiliary winding	207
Fig. 8.4	Transient performance of exhaust fan motor at full load (a) Supply voltage and voltages across main winding, auxiliary winding and capacitor, (b) Supply voltage, supply current, main winding current and auxiliary winding current	208
Fig. 8.5	MATLAB Simulink based phase variable model for unsymmetrical permanent capacitor SPIM	213
Fig. 8.6	Transient performance of exhaust fan motor with phase variable model (a), Starting from zero to full speed, (b) At steady state	213
Fig. 8.7	MATLAB Simulink based d-q model for unsymmetrical permanent capacitor SPIM	216
Fig. 8.8	Transient performance of exhaust fan motor with d-q variables (a), Starting from zero to full speed, (b) At steady state	216
Fig. 8.9	Flowchart for optimal design of exhaust fan motor	226
Fig. 8.10	Meshing of FEA model in (a) 2D and (b) 3D	230
Fig. 8.11	Performance of optimal design using FEA (a) Torque versus speed characteristics of motor and load, (b) Steady state supply current winding currents, (c) Flux density distribution in 2D FEA, (d) Flux density distribution using 3D	232
Fig. A.1	Equivalent circuit at no load and block rotor conducted on main winding keeping the auxiliary winding open from [165]	254
Fig. A.4	Equivalent circuit at rated condition from [73, 165]	261

Fig. B.1	Overall Arrangement of Parts for Calibration of Torque Transducer	269
Fig. B.2	Dimensions of arm side rod	270
Fig. B.3	Dimensions of the clamp-side holder	270
Fig. B.4	Dimensions of the torque transducer	271

## LIST OF TABLES

Table 3.1	Energy-Efficient Motor Specifications and Rated Parameters	42
Table 3.2	Calculated Equivalent Circuit Parameter Values	43
Table 3.3	Torque Sensor Calibration Readings	50
Table 3.4	Torque Sensor Calibration Readings	53
Table 3.5	Design Data of Energy-Efficient Ceiling Fan SPIMs for FEA Validation	55
Table 3.6	Steady-State Performance with Blade Characteristics	58
Table 3.7	No load and Block Rotor Test Results of Sample Motors	75
Table 3.8	Load Test Results and Calculated Output Power of Sample Motors	78
Table 4.1	Performance of 16 Pole Ceiling Fan Motor With Resistive Speed Controller	94
Table 4.2	Performance of 14 Pole Ceiling Fan Motor With Resistive Speed Controller	94
Table 4.3	Performance of 16 Pole Ceiling Fan Motor With Capacitive Speed Controller	101
Table 4.4	Performance of 14 pole Ceiling Fan Motor With Capacitive Speed Controller	101
Table 4.5	Performance of 16 Pole Ceiling Fan Motor With TRIAC Based Speed Controller	113
Table 4.6	Performance of 16 Pole Ceiling Fan Motor With TRIAC Based Speed Controller	114
Table 5.1	Rating and Performance Data of Existing 16 Pole Motor (FEA)	118
Table 5.2	Levels for Design Variables for L18 Orthogonal Array	123
Table 5.3	Design of L18 Orthogonal Arrays and Results	123
Table 5.4	Response Table for Means of First L18 OA	126
Table 5.5	Response Table for Means of Second L18 OA	126
Table 5.6	Levels For L4 and L8 OAs	127
Table 5.7	Design of Orthogonal Array for L4	127
Table 5.8	Response Table for Means of L4	127
Table 5.9	Design of Orthogonal Array for L8	128
Table 5.10	Response Table for Means of L8 OA	128
Table 5.11	Final Design Variations	129
Table 5.12	Design Data for Prototyping (First Design)	130
Table 5.13	Design Data for Prototyping (Second Design)	132
Table 5.14	Design Data for Prototyping (Third Design)	139
Table 5.15	Simulated Performance of Finalized Design	145
Table 5.16	Experimental Performance of Prototype and Comparison with Existing Motor	145
Table 5.17	Simulated Performance of Finalized Design	149

Table 5.18	Experimental Performance of Prototype and Comparison With Existing Motor	150
Table 5.19	Simulated Performance of Finalized Design	155
Table 5.20	Experimental Performance of Prototype and Comparison With Existing Motor	156
Table 6.1	Rating and Performance Data of Existing 14 Pole Motor (FEA)	161
Table 6.2	Design Data for 14 Pole Energy-Efficient Ceiling Fan Motors	173
Table 6.3	Simulated Performance of Finalized Design With 200 mm OD	174
Table 6.4	Simulated Performance of Finalized Design With 220 mm OD	177
Table 6.5	Cost Comparison of Existing Ceiling Fan With Low Cost High Speed Ceiling Fans	180
Table 7.1	Fixed Design Data for AFSPIM Optimization	194
Table 7.2	Stator and Rotor Slot Dimensions	194
Table 7.3	Design Data of Optimal Design of Ceiling Fan AFSPIM	199
Table 7.4	Rated Performance of Optimal Design from Analytical Solution and 3D FEA	199
Table 7.5	Comparison of Cost of AFSPIM and Weight with Existing Motor	201
Table 8.1	Design Specifications of Exhaust Fan Motor	206
Table 8.2	Performance Parameter of Existing Exhaust Fan	206
Table 8.3	Calculated Equivalent Circuit Parameter Values of Exhaust Fan	206
Table 8.4	Fixed Design Data for Optimization of Exhaust Fan SPIM	225
Table 8.5	Design Specifications of Exhaust Fan Motor	231
Table 8.6	Performance of Optimal Design Motor	231
Table 8.7	Comparison of Weight of Optimal Design	233

## LIST OF ABBREVIATIONS

AC	Alternating Current
AFSPIM	Axial Flux Single Phase Induction Motor
BLDC	Brushless Direct Current Motor
CMM	Cubic Meter Per Minute
DC	Direct Current
DoE	Design of Experiments
EMF	Electro-Motive Force
FEA	Finite Element Analysis
FF	Fil Factor
ID	Inner Diameter
MMF	Magneto-Motive Force
OA	Orthogonal Array
OD	Outer Diameter
pf	Power Factor
PM	Permanent Magnet
PMSM	Permanent Magnet Synchronous Motor
RFSPIM	Radial Flux Single Phase Induction Motor
SPIM	Single Phase Induction Motor

## LIST OF SYMBOLS

$A_b$	Rotor Bar Area
$A_{Aux}$	Auxiliary Winding Slot Area
$A_{Main}$	Main Winding Slot Area
$\alpha_{skew}$	Rotor Bar Skewing Angle
$b_{os1}$	Main Winding Slot Opening Width
$b_{os2}$	Auxiliary Winding Slot Opening Width
$B_{gav}$	Average Flux Density
$B_{t,aux}$	Average Flux Density of Auxiliary Winding Teeth
$B_{t,main}$	Average Flux Density of Main Winding Teeth
$C$	Capacitor in Series with Auxiliary Winding
$D$	Diameter of the Airgap
$D_b$	End Ring Mean Diameter
$D_{ro}$	Outer Diameter of the Rotor
$D_{ri}$	Inner Diameter of the Rotor
$D_{so}$	Outer Diameter of the Stator
$D_{si}$	Inner Diameter of the Stator
$G_a$	Wire Gauge of Auxiliary Winding
$G_m$	Wire Gauge of Main Winding
$h_e$	End Ring Height
$i_{as}$	Current in stator phase a
$i_{bs}$	Current in stator phase b
$i'_{ar}$	Current in rotor phase a referred to stator phase a
$i'_{br}$	Current in rotor phase b referred to stator phase b
$J$	Moment of Inertia of Motor
$L_{st}$	Stack Height of the Motor
$l_g$	Airgap Length Per Side
$\lambda_{as}$	Flux linkage of stator phase a
$\lambda_{bs}$	Flux linkage of stator phase b
$\lambda'_{ar}$	Flux linkage of rotor phase a referred to stator phase a
$\lambda'_{br}$	Flux linkage of rotor phase b referred to stator phase b

$L_{ss}$	Self inductance of stator phase a
$L_{SS}$	Self inductance of stator phase b
$L'_{rr}$	Self inductance of rotor phase a referred to stator phase
$L'_{rR}$	Self inductance of rotor phase b referred to stator phase
$L_{ms}$	Magnetizing inductance of stator phase a
$L_{mS}$	Magnetizing inductance of stator phase b
$N_a$	Turns in Auxiliary Winding
$N_m$	Turns in Main Winding
$N_r$	Rated Speed of the Rotor
$N_R$	Number of Rotor Bars
$P$	Number of Poles of Motor
$\sigma_{al}$	Conductivity of Aluminium
$\sigma_{Cu}$	Conductivity of Copper
$T_e$	Electromagnetic Torque
$v_{as}$	Voltage applied to stator phase a
$v_{bs}$	Voltage applied to stator phase b
$v'_{ar}$	Voltage applied to rotor phase a referred to stator phase a
$v'_{br}$	Voltage applied to rotor phase b referred to stator phase b
$v_C$	Voltage across capacitor
$w_e$	End Ring Width
$W_{t,aux}$	Width of the Auxiliary Winding Teeth
$W_{t,main}$	Width of the Main Winding Teeth
$w_{tr}$	Rotor Teeth Width